

Morphology control of inkjet-printed small-molecule organic thin-film transistors with bank structures

Yong-Hoon Kim^a and Sung Kyu Park^{b*}

^aFlexible Display Research Center, Korea Electronics Technology Institute, Seongnam, Gyeonggi 463-816, Republic of Korea

^bSchool of Electrical and Electronics Engineering, College of Engineering, Chung-Ang University, Seoul 156-756, Republic of Korea

(Received 26 April 2011; Revised 23 August 2011; Accepted 25 August 2011)

Reported herein is the film morphology control of inkjet-printed 6,13-bis(triisopropylsilylethynyl) pentacene (TIPS-pentacene) organic thin-film transistors for the improvement of their performance and of the device-to-device uniformity. The morphology of the inkjetted TIPS-pentacene films was significantly influenced by the bank geometry such as the bank shapes and confinement area for the channel region. A specific confinement size led to the formation of uniform TIPS-pentacene channel layers and better electrical properties, which suggests that the ink volume and the solid concentration of the organic-semiconductor solutions should be considered in designing the bank geometry.

Keywords: TIPS-pentacene; inkjet printing; morphology; bank structure

1. Introduction

The rapidly growing interest in flexible printed electronics, including flexible flat panel displays and printed electronics, has been the primary driving force for the development of organic thin-film transistors (OTFTs). The suitability of organic materials due to their good flexibility and low-temperature processing has made these technologies the focus of interest, and the continued development of organic semiconductors and processing technologies has induced much improvement in the OTFT performance and manufacturing process [1–6]. In particular, OTFTs with a variety of small-molecule organic materials on rigid and flexible substrates with record mobility have been reported [7–10]. The processing and characterization of materials for high-performance small-molecule OTFTs were initially developed using test structures on oxidized single crystal silicon wafers. The improvements in the processing and materials selection were transferred to glass or flexible polymeric substrates to demonstrate patterned gate OTFTs and simple OTFT circuits with performances suitable for several low-cost and large-area flexible electronics.

Organic electronics also attracted considerable interest in the electronic industry in the last decade due to their potential advantages for low-cost manufacturing and high-volume production. Their low-cost and high-volume production can open a new era in disposable

electronics. One way of reducing the manufacturing cost is to fabricate the electronics with solution-processed organic materials, using a cost-effective process. Therefore, several high-performance, soluble, small-molecule organic semiconductors with record mobility have been reported, using simple spin casting [11–15]. Spin casting may be a simple and effective solution process, but it also needs high material consumption, which may hinder the realization of its low-cost manufacturing. To overcome such limitations, the inkjet-printing technique has been considered a candidate for the cost-effective, volume-controllable, and highly selective patterning of the organic semiconductors [16].

The achievement of uniform and high-performance organic films from inkjet printing has been problematic, however, especially in small-molecule organic semiconductors, due to their complex drying mechanism such as the meniscus energy of the droplet ink, energy dissipation at the meniscus region, molecular diffusion in the solvents, and strong intermolecular interaction [17]. Reported herein is the improvement of inkjet-printed small-molecule OTFTs realized by employing simple bank structures and precise control of the volume density of the ink droplets. The key difference of and improvements in the technique proposed in this research over the previously proposed techniques lie in the easy control of the surface morphology and coverage with surface confinement for large-area printing technology application.

*Corresponding author. Email: skpark@cau.ac.kr

2. Experimental procedure

For simple bottom-contact-type OTFT device fabrication, a 200 nm thick layer of silicon dioxide was thermally grown as the gate dielectric on a heavily doped ($0.05 \Omega \text{ cm}$) n-type silicon wafer. The doped silicon wafer was used both as the sample substrate and as the gate electrode. Au source and drain (S/D) electrodes were deposited via thermal evaporation and were patterned using the lift-off process. The channel length and width of the devices were 10 and $50 \mu\text{m}$, respectively. Prior to the active layer deposition, the substrates were cleaned for 10 min via UV/ozone treatment. A self-assembled monolayer of pentafluorobenzenethiol (PFBT, Aldrich) was formed on the patterned Au source/drain electrodes to modify the organic-semiconductor microstructure and to improve the metal/organic contact and device performance. The PFBT monolayer was formed via immersion in a 1 mM ethanol solution for 15 min.

For bank fabrication, an acrylic-based negative-type photoresist was spin-coated and patterned via photolithography. The bank layer was $\sim 1.2 \mu\text{m}$ thick after baking at 180°C . Three types of bank structures were defined

(the circular, square, and rectangular types), with different dimensions, as described in Table 1, to examine the influence of bank shape and dimensions on the film morphology of the inkjet-printed organic semiconductor. After forming the bank structure, an organic semiconductor, 6,13-bis(triisopropylsilylethynyl) pentacene (TIPS-pentacene) (purchased from Sigma-Aldrich) solution, was inkjet-printed on the prepatterned bank structures and was dried. The TIPS-pentacene solution was formulated as 1 wt% in anisole. The inkjet printing of TIPS-pentacene was performed using a piezoelectric inkjet-printing system (UniJet UJ2100). The frequency of the jetting was 150 Hz, and the diameter of the ink drop was approximately $30\text{--}50 \mu\text{m}$ (ink volume: $14\text{--}65 \text{ pl}$).

3. Results and discussion

Although relatively high-performance TIPS-pentacene TFTs achieved through inkjet printing have been reported, the nonuniform morphology and electrical characteristics of TIPS-pentacene have been problematic. This nonuniformity is due mainly to the multiple nucleation and growth of TIPS-pentacene crystals during the drying process. To

Table 1. Electrical properties of the inkjet-printed TIPS-pentacene TFTs with different bank geometries

Bank type	Dimensions (area, μm^2)	Mobility ($\text{cm}^2 \text{ V}^{-1} \text{ s}^{-1}$)	$I_{\text{on/off}}$	V_{th} (V)	SS (V Decade $^{-1}$)
Circular	$D_C = 60 \mu\text{m}$ (2.8 k)	1.2×10^{-5}	8.26×10^3	6.0	1.22
	$D_C = 80 \mu\text{m}$ (5.0 k)	5.4×10^{-3}	2.37×10^6	0.2	1.01
	$D_C = 100 \mu\text{m}$ (7.9 k)	0.013	4.41×10^6	1.5	1.41
	$D_C = 120 \mu\text{m}$ (11.3 k)	0.033	3.90×10^6	-0.2	1.09
Square	$D_S = 60 \mu\text{m}$ (3.6 k)	5.3×10^{-3}	1.81×10^6	0.4	1.64
	$D_S = 80 \mu\text{m}$ (6.4 k)	7.4×10^{-3}	3.22×10^5	8.7	2.31
	$D_S = 100 \mu\text{m}$ (10.0 k)	0.017	3.64×10^6	3.8	1.21
Rectangular	$D_R = 60 \mu\text{m}, H = 120 \mu\text{m}$ (7.2 k)	0.027	6.16×10^6	0.2	1.35

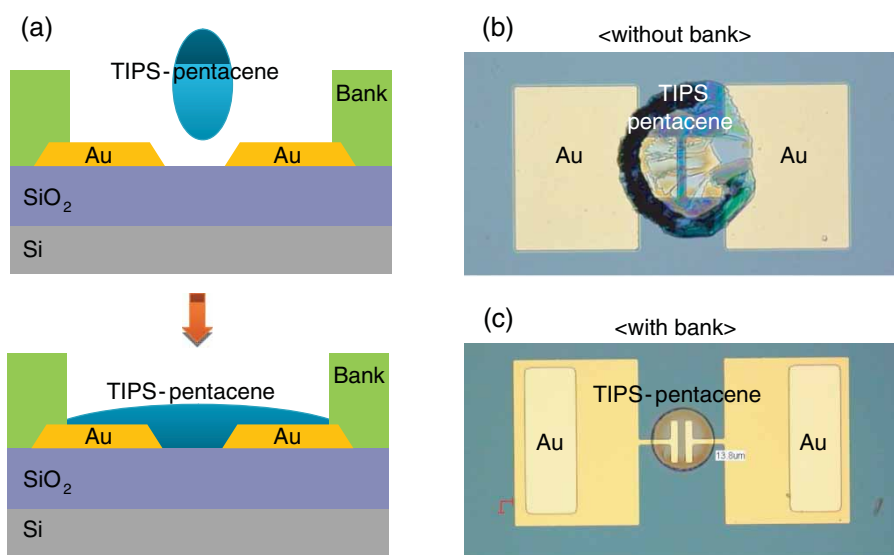


Figure 1. (a) Schematic diagrams of an inkjet-printed TFT with bank structure, and optical micrographs of inkjets printed TIPS-pentacene TFTs fabricated (b) without and (c) with bank structure.

avoid such effects and to obtain a uniform film morphology, a bank structure has been employed in the device structure, as shown in Figure 1(a). Without the bank structure to confine the dropped TIPS-pentacene ink, the inkjet-printed TIPS-pentacene film showed a nonuniform morphology (Figure 1b) of the multiple crystalline structures with a thicker outer channel region due to the coffee ring effect. Such nonuniformity may induce a serious problem, especially in large-area scale electronics. In contrast, by employing a bank structure, the TIPS-pentacene ink droplets are well confined to the predefined channel region, resulting in a uniform film morphology, as shown in Figure 1(c).

Using the bank structure to confine an ink droplet and to form an active channel layer, the shape and dimensions of the bank can be the key parameters for controlling the channel morphology. Three types of bank structures have been defined: the circular, square, and rectangular types (Figure 2). The detailed bank dimensions are listed in Table 1. Onto these bank structures with Au S/D electrodes formed below them, TIPS-pentacene ink was dropped, and the resulting film morphologies are shown in Figure 3. In the case of the circular bank structures, the bank diameter (D_C) of 60–100 μm typically showed nonuniform channel formation and poor coverage in the channel region (in the area between the S/D electrodes). Particularly, the growth of small crystals along the edges of the bank structure was observed, and a very weak formation in the channel region was monitored. Increasing the bank diameter up to 120 μm resulted in the formation of a uniform channel layer over the whole bank region. A similar behavior was observed in

the square bank structure. A nonuniform growth of small crystals was observed when the bank dimension (D_S) was 60–80 μm , whereas increasing the dimension to 100 μm led to the formation of a uniform channel layer. In the case of the rectangular bank structure, uniform channel layers were obtained with the dimensions of 60 μm length (D_R) and 120 μm height (H).

In Figure 4, the transfer characteristics of TIPS-pentacene TFTs fabricated with different bank structures are shown. Moreover, the extracted electrical properties are listed in Table 1. As expected from the observed film morphologies, the TFTs with uniform channel layers showed better electrical properties. In the case of the circular bank structure, the 120 μm diameter showed the highest field effect mobility ($0.033 \text{ cm}^2 \text{ V}^{-1} \text{ s}^{-1}$). Moreover, in the case of the square bank structure, the 100 μm diameter showed the highest field effect mobility ($0.017 \text{ cm}^2 \text{ V}^{-1} \text{ s}^{-1}$). With the rectangular bank structure, a field effect mobility of $0.027 \text{ cm}^2 \text{ V}^{-1} \text{ s}^{-1}$ was observed, with $L = 60 \mu\text{m}$ and $W = 120 \mu\text{m}$. Figure 5 summarizes the dependence of the field effect mobility on the bank shape and dimension (bank area).

From the experiments described above, it was noted that the relatively low performance in the smaller bank structure is possibly due to the nonuniform and multiple crystal growth at the bank edges. With a fixed volume of TIPS-pentacene ink supplied to the channel area, a higher concentration of TIPS-pentacene molecules is expected with the smaller bank structures. In this case, multiple crystal seeds can be grown from the edges (at the interface of the gate dielectric and the bank layer), and as a consequence,

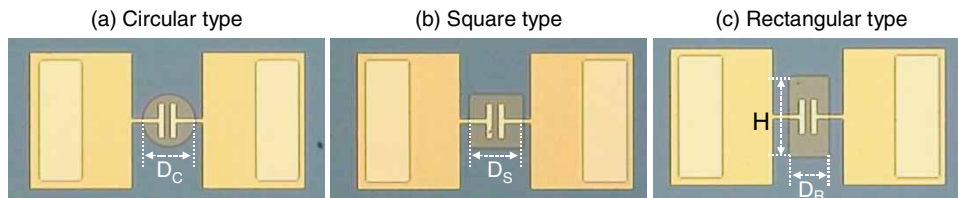


Figure 2. Optical micrographs of the fabricated TIPS-pentacene TFTs with different bank structures: (a) circular type, (b) square type, and (c) rectangular type.

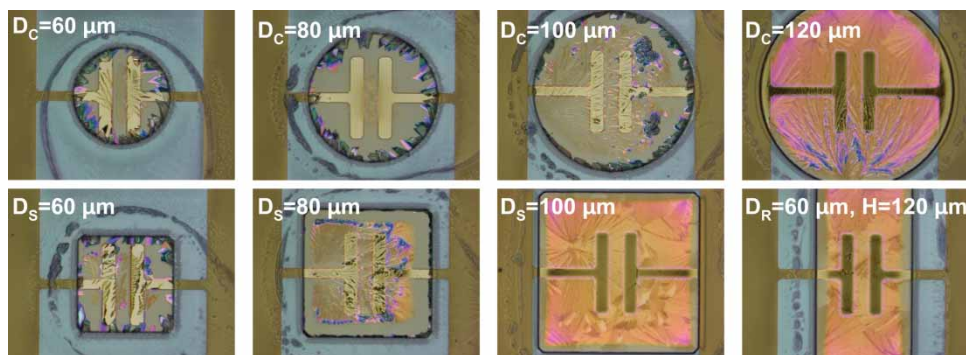


Figure 3. Morphologies of the inkjet-printed TIPS-pentacene films with different bank shapes and dimensions: (i) circular type—diameter (D_C) = 60, 80, 100, and 120 μm ; (ii) square type—length (D_S) = 60, 80, and 100 μm ; and (iii) rectangular type—length (D_R) = 60 μm and height (H) = 120 μm .

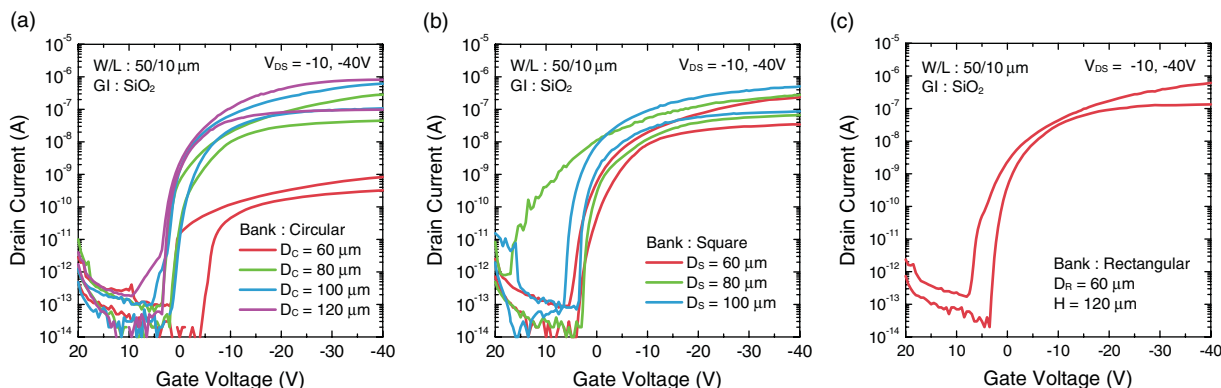


Figure 4. Transfer characteristics of the inkjet-printed TIPS-pentacene TFTs with different bank structures. The channel length and width of the TFTs were 10 and 50 μm , respectively.

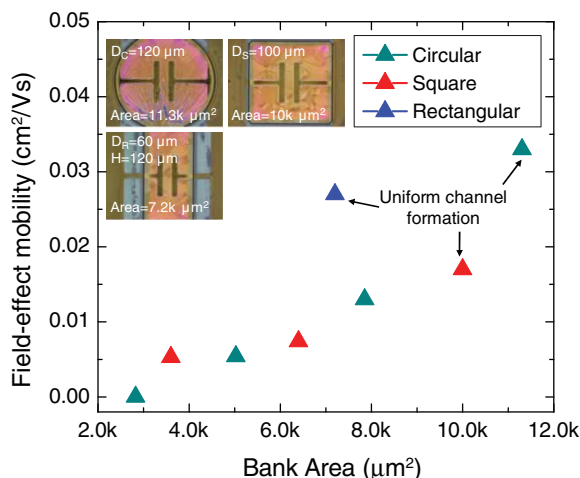


Figure 5. Dependence of the field effect mobility on the bank shape and dimension (area). The field effect mobility was obtained with a gate voltage of -40 V .

a nonuniform channel is expected to be formed. Although the crystals growing from the edges propagate towards the center of the bank region, the actual channel region of the transistor (the gap between the source and drain electrodes) is not fully covered by the organic-semiconductor crystals because the TIPS-pentacene molecules are already consumed by forming multiple crystals at the edges. In contrast to the results of the OTFTs with small bank structures and with appropriate bank sizes ($\sim 100\ \mu\text{m}$), the TIPS-pentacene ink is well spread over the channel area, and a uniform channel layer is formed, with a relatively high performance. With the uniform channel layers, field effect mobilities of $0.017\text{--}0.033\ \text{cm}^2\ \text{V}^{-1}\ \text{s}^{-1}$ were obtained with various bank structures. Increasing the dimensions of the predefined bank structures typically led to nonuniform and discontinuous-film formation due to the lack of TIPS-pentacene molecules supplied to the channel region. Therefore, in the case of employing predefined bank structures, the dimensions of the bank structures should be decided considering the ink volume and solid concentration of the organic-semiconductor solutions.

4. Conclusions

The effects of the bank structure on the morphology of the inkjet-printed TIPS-pentacene channel layer and on the electrical properties of TFT devices were evaluated, and it was found that the film morphology and coating uniformity of the inkjet-printed TIPS-pentacene film can be controlled through the geometry of the predefined bank structure. Uniform channel layers were formed using specific bank dimensions, suggesting that the bank geometry should be designed considering the ink volume and solid concentration of the organic-semiconductor solutions.

Acknowledgements

This work was supported in part by the Basic Science Research Program through a National Research Foundation of Korea (NRF) grant funded by the Ministry of Education, Science, and Technology (No. 2010-0002623).

References

- [1] S.E. Burns, W. Reeves, B.H. Pui, K. Jacobs, S. Siddique, K. Reynolds, M. Banach, D. Barclay, K. Chalmers, N. Cousins, P. Cain, L. Dassel, M. Etchells, C. Hayton, S. Markham, A. Menon, P. Too, C. Ramsdale, J. Herod, K. Saynor, J. Watts, T. von Werne, J. Mills, C.J. Curling, H. Siringhaus, K. Amundson, and M.D. McCreary, *SID Tech. Dig.* **74** (2006).
- [2] Y.H. Kim, S.K. Park, D.G. Moon, W.K. Kim, and J.I. Han, *Jpn. J. Appl. Phys.* **43**, 3605 (2004).
- [3] J.B. Chang, V. Liu, and V. Subramanian, *J. Appl. Phys.* **100**, 014506 (2006).
- [4] T. Someya, T. Sekitani, S. Iba, Y. Kato, H. Kawaguchi, and T. Sakurai, *PNAS* **101**, 9966 (2004).
- [5] V. Subramanian, J.M.J. Frechet, P.C. Channg, D.C. Huang, J.B. Lee, S.E. Molesa, A.R. Murphy, D.R. Redinger, and S.K. Volkman, *Proc. IEEE* **93**, 1330 (2005).
- [6] S.R. Forrest, *Nature* **428**, 911 (2004).
- [7] K. Takimiya, H. Ebata, K. Sakamoto, T. Izawa, T. Otsubo, and Y. Kunugi, *J. Am. Chem. Soc.* **128**, 12604 (2006).
- [8] M.M. Payne, S.R. Parkin, J.E. Anthony, C.-C. Kuo, and T.N. Jackson, *J. Am. Chem. Soc.* **127**, 4986 (2005).

- [9] D. Kumaki, T. Umeda, T. Suzuki, and S. Tokito, *Org. Elec.* **9**, 921 (2008).
- [10] H. Klauk, U. Zschieschang, R.T. Weitz, H. Meng, F. Sun, G. Nunes, D.E. Keys, C.R. Fincher, and Z. Xiang, *Adv. Mater.* **19**, 3882 (2007).
- [11] S.K. Park, T.N. Jackson, J.E. Anthony, and D.A. Mourey, *Appl. Phys. Lett.* **91**, 063514 (2007).
- [12] D.H. Kim, D.Y. Lee, H.S. Lee, W.H. Lee, Y.H. Kim, J.I. Han, and K. Cho, *Adv. Mater.* **19**, 678 (2007).
- [13] J.P. Hong and S. Lee, *Angew. Chem.* **121**, 3142 (2009).
- [14] D.J. Gundlach, J.E. Royer, S.K. Park, S. Subramanian, O.D. Jurchescu, B.H. Hamadani, A.J. Moad, R.J. Kline, C.L. Teague, O. Kirillov, C.A. Richter, J.G. Kushmerick, L.J. Richter, S.R. Parkin, T.N. Jackson, and J.E. Anthony, *Nature Mater.* **7**, 216 (2008).
- [15] Y. Li, Y. Wu, P. Liu, Z. Prostran, S. Gardner, and B.S. Ong, *Chem. Mater.* **19**, 418 (2007).
- [16] D.H. Song, M.H. Choi, J.Y. Kim, J. Jang, and S. Kirchmeyer, *Appl. Phys. Lett.* **90**, 053504 (2007).
- [17] J.A. Lim, W.H. Lee, H.S. Lee, J.H. Lee, Y.D. Park, and K. Cho, *Adv. Funct. Mater.* **18**, 229 (2008).